AGU PUBLICATIONS

Geophysical Research Letters

RESEARCH LETTER
10.1002/2016GL068020

The overlooked tropical oceanic CO_2 sink

J. Severino P. Ibánhez[1], **Moacyr Araujo**[1], **and Nathalie Lefèvre**[1,2]

[1]Department of Oceanography–DOCEAN, Federal University of Pernambuco–UFPE, Recife, Brazil, [2]IRD-LOCEAN, Sorbonne Universités (Université Pierre et Marie Curie-CNRS-MNHN), Paris CEDEX 05, France

Key Points:
- The Amazon plume area has been overestimated in >16% due to rainfall
- The atmospheric CO_2 sink associated to the Amazon plume is of global importance
- The sea-air CO_2 exchange for the tropical Atlantic needs reevaluation

Supporting Information:
- Supporting Information S1

Correspondence to:
J. S. P. Ibánhez,
pinoibaj@tcd.ie

Citation:
Ibánhez, J. S. P., M. Araujo, and N. Lefèvre (2016), The overlooked tropical oceanic CO_2 sink, *Geophys. Res. Lett.*, *43*, 3804–3812, doi:10.1002/2016GL068020.

Received 28 JAN 2016
Accepted 29 MAR 2016
Accepted article online 5 APR 2016
Published online 18 APR 2016

Abstract The intense rainfall in the tropical Atlantic spatially overlaps with the spread of the Amazon plume. Based on remote-sensed sea surface salinity and rainfall, we removed the contribution of rainfall to the apparent Amazon plume area, thus refining the quantification of its extension ($0.84 \pm 0.06 \times 10^6$ km^2 to $0.89 \pm 0.06 \times 10^6$ km^2). Despite the previous overestimation of the Amazon plume area due to the influence of rainfall (>16%), our calculated annual CO_2 flux based on rainfall-corrected sea surface CO_2 fugacity confirms that the Amazon River plume is an atmospheric CO_2 sink of global importance (-7.61 ± 1.01 to -7.85 ± 1.02 Tg C yr^{-1}). Yet we show that current sea-air CO_2 flux assessments for the tropical Atlantic could be overestimated in about 10% by neglecting the CO_2 sink associated to the Amazon plume. Thus, including the Amazon plume, the sea-air CO_2 exchange for the tropical Atlantic is estimated to be 81.1 ± 1.1 to 81.5 ± 1.1 Tg C yr^{-1}.

1. Introduction

Global oceans act as net sinks of atmospheric CO_2, thus mitigating the impact of the anthropogenic CO_2 emissions in the atmosphere [*Takahashi et al.*, 2009; *Landschützer et al.*, 2014]. Oceanic CO_2 sink areas are concentrated at high latitudes, while the tropical oceans generally act as sources of CO_2 to the atmosphere [*Takahashi et al.*, 2009; *Landschützer et al.*, 2014]. The tropical Atlantic is the second largest oceanic CO_2 source to the atmosphere after the tropical Pacific, accounting for an annual emission of 98–110 Tg C [*Takahashi et al.*, 2009; *Landschützer et al.*, 2014]. The zonal spread of CO_2-rich waters that originated in the equatorial upwelling system driven by the surface currents explains this net CO_2 outgassing [*Andrié et al.*, 1986]. Nevertheless, large, poorly studied areas of the tropical Atlantic surface are characterized by CO_2 undersaturation associated to freshwater sources to the basin [*Lefèvre et al.*, 2010], which rises doubts about current sea-air CO_2 estimations for the basin and the role of the tropical Atlantic in the global sea-air CO_2 exchange.

The Amazon River is the largest river in the world, accounting for almost 20% of the global river discharge onto the oceans [*Cai et al.*, 2013, and references therein]. In the Atlantic Ocean, the dispersal of Amazon River waters develops a brackish water plume that can exceed 10^6 km^2, reaching latitudes as far from the river mouth as 30°W [*Coles et al.*, 2013] or even 25°W when the North Equatorial Countercurrent (NECC) is strong [*Lefèvre et al.*, 1998]. The upper Amazon River is a large source of CO_2 to the atmosphere (210 ± 60 Tg C yr^{-1}) [*Richey et al.*, 2002], supported by organic matter mineralization and CO_2 and organic matter exportation from flooded wetlands [*Abril et al.*, 2014]. As it mixes with oceanic waters, high-nutrient concentrations transported by the river together with the progressive establishment of more favorable conditions (lower turbidity) stimulate primary producers' growth and associated biological carbon drawdown [*Chen et al.*, 2012]. The spread of Amazon waters in the tropical Atlantic is also known to support significant N_2 fixation, becoming the main pathway of C sequestration within the plume [*Subramaniam et al.*, 2008]. The sinking of C that originated in the primary production within the Amazon River plume is estimated to be 27.6 Tg C/yr [*Subramaniam et al.*, 2008]. Such C drawdown rapidly reverts the CO_2 saturation conditions of the Amazon waters and leads to a globally significant sink of atmospheric CO_2 [*Ternon et al.*, 2000; *Körtzinger*, 2003; *Cooley et al.*, 2007; *Lefèvre et al.*, 2010; *Ibánhez et al.*, 2015].

Here we reveal the systematic overlook of the role of the Amazon River plume in the current sea-air CO_2 exchange estimations for the tropical Atlantic. We present an improved estimation of the atmospheric CO_2 sink associated to the Amazon River plume based on extensive underway sea surface CO_2 fugacity (fCO_{2sw}) observations and high-resolution, novel remote-sensed sea surface salinity (SSS). The results obtained are used to requantify the net CO_2 outgassing associated to the tropical Atlantic.

2. Methods

An automated CO_2 analyzer similar to that described in *Pierrot et al.* [2009] was installed in 2006 on board the merchant ship Maritime Nantaise (MN) Colibri performing the route Le Havre (mainland France)-Kourou (French Guyana). The ship was also equipped with a Sea-Bird thermosalinograph for continuous sea surface temperature (SST; °C) and SSS measurements. From 2006 to 2013, 20 voyages of the MN Colibri recorded data within the Amazon River plume (Table S1 in the supporting information). fCO_2 (μatm) obtained from the Colibri tracks was used to develop a model of the fCO_2 in the Amazon River plume waters.

Monthly averaged atmospheric CO_2 mole fraction ($\times CO_{2atm}$, ppm) recorded at the station of the NOAA/Earth System Research Laboratory (ESRL) Global Monitoring Division closest to the Amazon River plume (Ragged Point, Barbados, 13.17°N, 59.43°W; http://www.esrl.noaa.gov/gmd/ccgg/iadv/) was used for the atmospheric fCO_2 (fCO_{2atm}) and sea-air CO_2 flux calculations. fCO_{2atm} was calculated as

$$fCO_{2atm} = xCO_{2atm}(P - pH_2O)C_f \tag{1}$$

where P is the atmospheric pressure (atm), pH_2O is the water vapor pressure at 100% humidity (atm) calculated from SST and SSS, and C_f is the fugacity coefficient calculated according to *Weiss* [1974]. Monthly atmospheric pressure from May 2010 to December 2014 was obtained from the National Centers for Environmental Prediction (NCEP)/National Center for Atmospheric Research Reanalysis project, initially at a 2.5° resolution, and linearly interpolated into the working grid (0.25°×0.25°). Monthly SST for the same period was derived from the daily NOAA optimum interpolation (OI) SST v2 data (0.25°×0.25°) [*Reynolds et al.*, 2002] provided by the NOAA/Oceanic and Atmospheric Research (OAR)/ESRL Physical Sciences Division (PSD), Boulder, CO, USA (http://www.esrl.noaa.gov/psd/) and averaged for each month. Monthly SSS data (0.25° resolution) derived from the Soil Moisture and Ocean Salinity (SMOS) mission were obtained from the Ocean Salinity Expertise Center (CECOS) of the Centre National d'Etudes Spatiales- Institut Français de Recherche pour l'Exploitation de la Mer (IFREMER) Centre Aval de Traitemenent des Données (CATDS), at IFREMER, Plouzané (France). The available monthly SSS composites (from May 2010 to December 2014) were used. Furthermore, available daily SSS products (0.5° resolution) of the SMOS mission were compared with SSS measured on board the MN Colibri. SSSs measured along the Colibri tracks south of 12°N were averaged for every pixel of the SMOS daily products.

Sea-air CO_2 fluxes (F; mmol m^{-2} d^{-1}) within the Amazon River plume were calculated according to

$$F = k \ \ S_o(fCO_{2sw} = fCO_{2atm}) \tag{2}$$

where S_o is the solubility of CO_2 (mol kg^{-1} atm^{-1}) as a function of SST and SSS [*Weiss*, 1974], k is the gas transfer velocity (m d^{-1}), and fCO_{2sw} is the fCO_2 of the surface ocean waters (calculated from that measured along the Colibri tracks). k was calculated according to Sweeney et al. [*Sweeney et al.*, 2007]:

$$k = 0.27 \ \ U_{10}^2(\mathrm{Sc}/660)^{-0.5} \tag{3}$$

where Sc is the Schmidt number and U_{10} is the wind speed (m d^{-1}) at 10 m above sea level. Monthly mean U_{10} from May 2010 to December 2014 was taken from the European Centre for Medium-Range Weather Forecasts reanalysis data set (ERA-Interim; 0.25° resolution).

Monthly Amazon River discharge (m^3 s^{-1}) from May 2010 to December 2014 was obtained from the Environmental Research Observatory HYBAM (Geodynamical, hydrological, and biogeochemical control of erosion/alteration and material transport in the Amazon basin; http://www.ore-hybam.org). Monthly zonal sea surface current velocities (cm s^{-1}) from May 2010 to December 2014 were downloaded from the Ocean Surface Current Analyses Real-time data, obtained from Jet Propulsion Laboratory Physical Oceanography Distributed Active Archive Center and developed by ESR (1° resolution). Additionally, monthly wind, Amazon River discharge, sea surface current velocity, and SST climatologies were computed for the period of 1995–2014. Monthly wind, Amazon River discharge, SST, and sea surface current velocity anomalies were then computed for the period covered in this study (2010–2014). Wind, SST, and sea surface current anomalies were integrated over the area 7.5–12.5°N and 45–55°W. These anomalies together with river discharge anomalies were used to elucidate the impact of the variability of these physical parameters in the Amazon plume area and calculated sea-air CO_2 exchange.

SSS in the western tropical Atlantic is strongly influenced by the Amazon River discharge, advection by surface currents, and rainfall [*Grodsky et al.*, 2014]. From December to May, the North Brazil Current (NBC) advects the

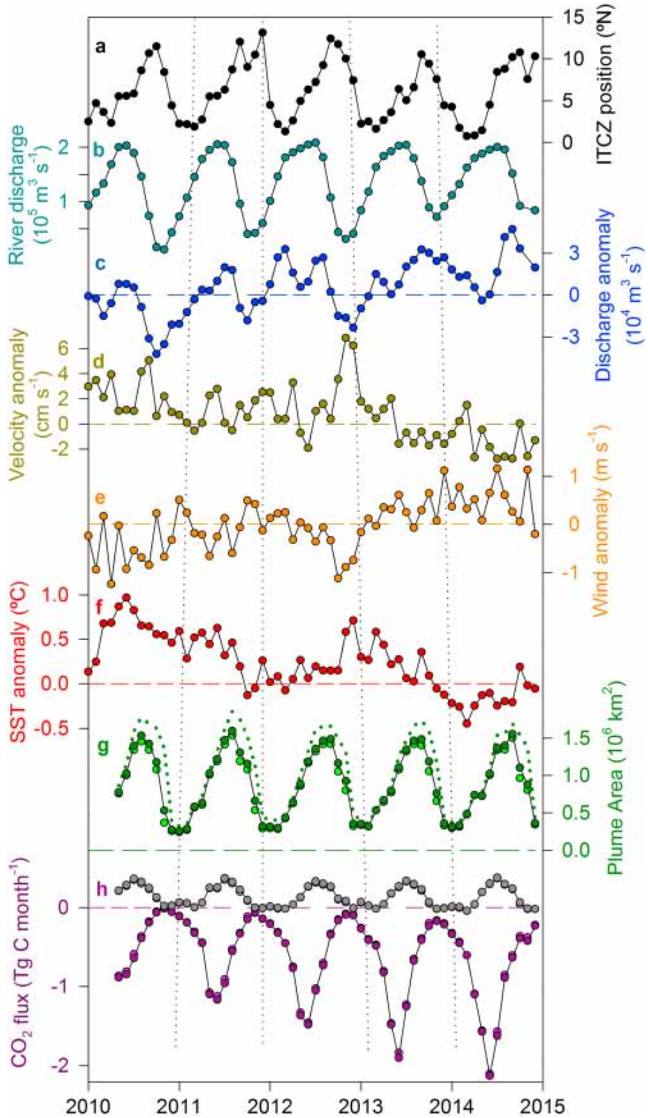

Figure 1. Monthly distribution of relevant properties in the area of the Amazon River plume. (a) Calculated ITCZ position. (b) Monthly Amazon River discharge. (c) Monthly Amazon River discharge anomalies. (d) Zonal surface water velocity anomalies. (e) Wind intensity anomalies. (f) SST anomalies. (g) Amazon River plume area. The dotted line represents the area with SSS lower than 35 psu, whereas the filled dots represent the calculated Amazon River plume after removing the influence of rainfall over SSS by using the conservative (dark green) and the high-end (light green) empirical SSS versus precipitation relationship found in the eastern tropical Atlantic. (h) Calculated monthly sea-air CO_2 fluxes in the Amazon River plume for the period covered by the SMOS mission. The dark (light) magenta represents the calculated monthly sea-air CO_2 fluxes using the conservative (high-end) rainfall versus SSS estimate. Furthermore, the monthly sea-air CO_2 fluxes for the Amazon River plume as calculated from the CO_2 flux climatology of *Landschützer et al.* [2014] are also shown in dark grey (grey).

Amazon waters along the northern coast of South America. From May to November, the NBC retroflection transports most of the Amazon waters eastward in the NECC along the 5 to 10°N latitudinal band [*Coles et al.*, 2013]. From July to November, most of the Amazon plume is transported eastward, coinciding with the northern most annual position of the Intertropical Convergence Zone (ITCZ) associated to intense rainfall. This spatial overlapping of both sources of freshwater develops a region of almost continuous surface brackish waters across the basin, thus increasing the apparent extension of the Amazon plume [*Coles et al.*, 2013; *Grodsky et al.*, 2014].

Monthly precipitation data sets (mm h^{-1}) obtained from the Tropical Rainfall Measuring Mission (TRMM) [*Huffman et al.*, 2007] (http://precip.gsfc.nasa.gov/; 0.25° resolution) were used to quantify the influence of the rainfall associated to the ITCZ on the freshening observed in the area of the Amazon plume and its influence on the resulting sea-air CO_2 exchange. Furthermore, the position of the ITCZ was calculated from the TRMM data as the monthly maximum precipitation latitudinal band within 0–24°N and averaged for the 60–30°W longitudinal band (Figure 1a).

Throughout this study, the errors associated to our results correspond to the standard error of the estimate.

3. Results and Discussion

3.1. SSS in the Western Tropical North Atlantic

Novel results from the SMOS mission permit for the accurate determination of SSS in the tropical Atlantic [*Grodsky et al.*, 2014]. The SMOS reanalysis products (available for the period of May 2010 to December 2014) have been extensively validated with in situ data, and for the tropical Atlantic, the estimated error is 0.33 practical salinity unit (psu) [*Hernandez et al.*, 2014]. Furthermore, SSS obtained from the daily SMOS products available for the Amazon plume area is in very good agreement with that measured along the Colibri tracks (slope = 0.993, $R = 0.93$, $n = 223$, $p < 0.001$; Figure S1 in the supporting information).

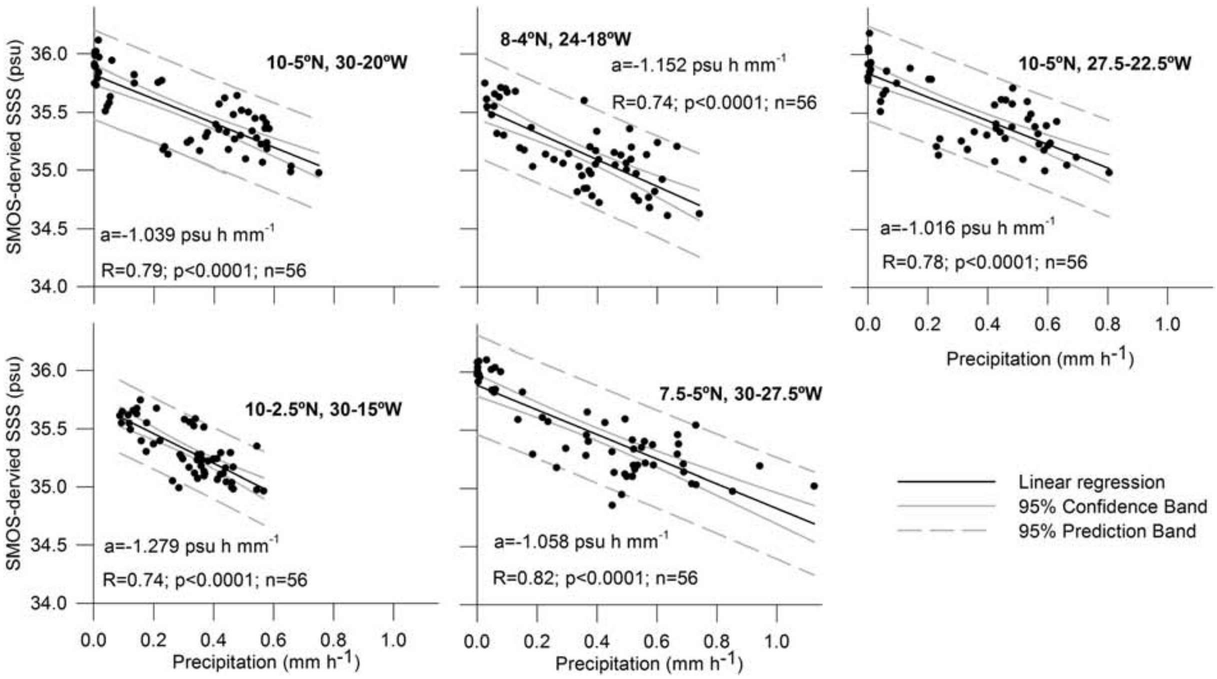

Figure 2. Rainfall influence over SSS in the tropical Atlantic. Comparison of SSS obtained from the SMOS monthly products and satellite-derived precipitation integrated over different areas within the tropical North Atlantic and in the latitudinal band seasonally influenced by the ITCZ. The resulting linear regression and the 95% confidence and prediction bands are also shown.

We compared the monthly precipitation rate with monthly SSS in five regions of the tropical Atlantic with the ITCZ as the only freshening source to elucidate the contribution of rainfall to the bulk freshening observed in the area of the Amazon plume (Figure 2). Despite the seasonality and spatial heterogeneity of climatic and hydrodynamic forces that determine the mixed layer depth and consequently its salinity balance in the tropical Atlantic [*Da-Allada et al.*, 2013], we found highly significant linear relationships of precipitation with SSS across the basin ($R > 0.73$, $n = 56$, $p < 0.0001$, slope from 1.016 to 1.279 psu h mm^{-1}; Figure 2). We used the lower slope (1.016 psu h mm^{-1}) of the SSS versus precipitation relationships found together with rainfall rate to conservatively estimate the influence of rainfall over the measured SSS in the tropical Atlantic region affected by the Amazon plume (results derived from the use of the higher slope, 1.279 psu h mm^{-1}, are also shown in brackets for comparison). The Caribbean Sea was excluded from this analysis to limit the influence of the Orinoco waters [*Grodsky et al.*, 2014]. After removing the freshening caused by rainfall, the area of the western tropical Atlantic (61–31°W) with SSS <35 psu (hereby defined as the Amazon River plume) was reduced by 16.6 ± 1.5% (range 3.2–61.1%, $n = 56$; Figure 1g) [20.6 ± 1.8% on the high-end estimate, range 3.6–73.0%, $n = 56$]. This is the first time that the rainfall contribution has been separated from the freshening caused by the Amazon River dispersal in the tropical Atlantic.

After removing the influence of rainfall in the freshening observed in the western tropical Atlantic, the areal extension of the Amazon River plume was still highly significant, ranging from 0.25 to 1.60×10^6 km^2 (average $0.89 \pm 0.06 \times 10^6$ km^2; Figure 1g) [from 0.24 to 1.54×10^6 km^2 on the high-end estimate, average $0.84 \pm 0.06 \times 10^6$ km^2]. Previous estimations of the extension of the Amazon plume were based on bulk SSS data and therefore did not account for the freshening caused by the ITCZ in the area. Based on SSS obtained from the World Ocean Atlas 2001 and 2005, *Körtzinger* [2003] and *Lefèvre et al.* [2010] estimated the area of the Amazon plume in 2.4×10^6 km^2 and 1.1×10^6 km^2, respectively. The intense rainfall associated to the ITCZ has very likely led to a significant overestimation of the spatial extension of the Amazon River plume in previous studies.

The Amazon River plume area showed high seasonal variability, according to the seasonality of the main processes responsible for its spread in the tropical Atlantic (river discharge, wind intensity, and the magnitude of the local system of surface currents [*Molleri et al.*, 2010]). The Amazon plume area generally peaked during August (1.49 ± 0.03 [1.43 ± 0.03] $\times 10^6$ km^2), reaching longitudes as far from the river mouth as 32°W coincident with the period of the NBC retroflection. This period of the year coincides with the northernmost transport of Amazon waters driven by Ekman currents and eddies [*Mignot et al.*, 2012], reaching latitudes higher than 22°N. Despite this strong seasonality, no significant interannual changes in the Amazon plume area were observed among the five studied years ($p > 0.2$; Figure 1g). A general linear model (GLM) of wind intensity ($p < 0.001$) and river discharge ($p < 0.001$) significantly explained the variability of the Amazon River plume for both the conservative and the high-end estimates of the influence of rainfall ($R^2 = 0.84$ [$R^2 = 0.84$], $n = 56$).

3.2. fCO_{2sw} in the Amazon River Plume

The Amazon River plume is the main driver of the fCO_{2sw} variability in the western tropical Atlantic. fCO_{2sw} determined along the tracks of the merchant ship MN Colibri (Figure S2 in the supporting information) within the Amazon River plume ranged from 122.9 to 411.4 μatm for the period of 2006–2013. During this period, atmospheric fCO_2 averaged 375 μatm along the Colibri tracks, which pictures the strong CO_2 undersaturation commonly found within the plume [*Ternon et al.*, 2000; *Körtzinger*, 2003; *Cooley et al.*, 2007; *Lefèvre et al.*, 2010; *Ibánhez et al.*, 2015]. fCO_{2sw} within the Amazon River plume as measured along the Colibri tracks was significantly correlated with SSS ($fCO_{2sw} = 15.5$ (±0.1) SSS − 158.5 (±3), $R = 0.9$, $n = 6016$; *Ibánhez et al.*, 2015), consistent with previous studies in the area [*Ternon et al.*, 2000; *Körtzinger*, 2003; *Lefèvre et al.*, 2010]. Comparison of the correlation between fCO_{2sw} and SSS within the Amazon plume as measured along the Colibri tracks with previously published relationships can be found in *Ibánhez et al.* [2015].

Rainfall impacts the physics and chemistry of the surface waters, thus altering the inorganic C chemistry and the CO_2 transfer between the ocean and the atmosphere [*Turk et al.*, 2010]. The relationships of rainfall versus SSS changes in the tropical Atlantic allow us to estimate the effect of rainfall over fCO_{2sw} within the plume. Since rainfall usually contains zero TAlk and near-zero dissolved inorganic C (DIC), chemical dilution of TAlk and DIC and atmospheric DIC deposition are the main effects of rainfall over the observed fCO_{2sw} [*Sarmiento and Gruber*, 2006; *Turk et al.*, 2010]. Assuming constant temperature, the change in fCO_{2sw} due to rainfall can be calculated as [*Sarmiento and Gruber*, 2006]

$$\Delta f\mathrm{CO}_{2\mathrm{sw}} = \Delta \mathrm{SSS}\frac{\partial f\mathrm{CO}_{2\mathrm{sw}}}{\partial \mathrm{SSS}} + \Delta \mathrm{DIC}\frac{\partial f\mathrm{CO}_{2\mathrm{sw}}}{\partial \mathrm{DIC}} + \Delta \mathrm{TAlk}\frac{\partial f\mathrm{CO}_{2\mathrm{sw}}}{\partial \mathrm{TAlk}} \quad (4)$$

We interpolated the monthly rainfall data at the position where measurements on board MN Colibri were performed within the Amazon plume and used the SSS versus rainfall relationships presented here to obtain the change in SSS caused by rainfall. Furthermore, we used the global mean values of the sensitivity of fCO_{2sw} to changes in DIC and TAlk and the salinity dependence of fCO_{2sw} [*Sarmiento and Gruber*, 2006] to calculate the theoretical fCO_{2sw} in the Amazon plume without rainfall (Figure S3 in the supporting information). The theoretical relationship between fCO_{2sw} and SSS in the Amazon plume without rainfall becomes $fCO_{2sw} = 15.9$ (±0.1) SSS − 171.3 (±3.4), $R = 0.9$, $n = 5642$ (Figure S3 in the supporting information) [$fCO_{2sw} = 16.1$ (±0.1) SSS − 177.1 (±3.5), $R = 0.9$, $n = 5504$ on the high-end estimate].

3.3. Sea-Air CO_2 Fluxes in the Amazon River Plume

The theoretical fCO_{2sw} model developed here for the Amazon River plume after removing the effect of rainfall was used together with SMOS-derived SSS (after removing the contribution of rainfall to the observed freshening in the area) and optimum interpolation SST products to calculate the sea-air CO_2 exchange in the Amazon River plume. The lowest SSS used in the fCO_{2sw} model (17.4 psu) was used as the lower boundary of the fCO_{2sw} extrapolation. Calculated monthly sea-air CO_2 fluxes within the Amazon plume ranged from −2.12 to 0.01 Tg C month^{-1} (−2.10 to −0.02 Tg C month^{-1} for the high-end estimate) for the studied period (Figure 1h), where negative CO_2 fluxes denote sea surface CO_2 absorption. A GLM with month ($p < 0.01$), river discharge ($p < 0.001$), wind intensity ($p < 0.001$), and plume area ($p < 0.001$) significantly explained the variability of the calculated CO_2 fluxes in the Amazon plume ($R^2 = 0.83$ [$R^2 = 0.82$], $n = 56$).

Maximum atmospheric CO_2 absorption (more negative CO_2 flux values) within the plume systematically occurred during May–June (Figure 1h), when the monthly discharge of the river peaks (Figure 1b). Overall, net monthly CO_2 outgassing in the Amazon River plume was only verified during September to November 2010. Year 2010 was a year of significant climatic changes in the tropical Atlantic following the 2009 Pacific El Niño [*Richter et al.*, 2013], which led to an increased CO_2 outgassing in the basin [*Lefèvre et al.*, 2013]. In the Amazon plume area, 2010 was characterized by the highest positive SST (Figure 1f) and negative wind intensity (Figure 1e) and river discharge (Figure 1c) anomalies of the studied period. Thus, the reduced atmospheric CO_2 absorption in the Amazon plume during 2010 contributed to the increased CO_2 outgassing observed in the tropical Atlantic during that period.

Excluding the anomalous year 2010, the calculated mean annual sea-air CO_2 flux in the Amazon River plume was -7.85 ± 1.02 Tg C yr^{-1} (from -5.57 Tg C in 2011 to -10.40 Tg C in 2014) [-7.61 ± 1.01 Tg C yr^{-1}; from -5.35 Tg C in 2011 to -10.12 Tg C in 2014 for the high-end estimate], in accordance with previous CO_2 flux estimations for the Amazon River plume (from -5 to -15 ± 6 Tg C/yr [*Körtzinger*, 2003; *Cooley et al.*, 2007; *Lefèvre et al.*, 2010]). *Körtzinger* [2003] and *Lefèvre et al.* [2010] based their estimations on empirical linear relationships of fCO_{2sw} with SSS within the river plume. *Cooley et al.* [2007] based their estimation on the extrapolation of calculated CO_2 fluxes for the area of the Amazon plume determined from the Sea-viewing Wide Field-of-view Sensor satellite data. In all cases, these estimations were based on bulk SSS in the western tropical Atlantic. We further used the linear relationship between fCO_{2sw} and SSS found by *Ibánhez et al.* [2015] with SMOS-derived bulk SSS for the area 31–61°W and 5°S–22°N (i.e., not removing the freshening effect of rainfall in the region). The resulting annual CO_2 flux (from 2011 to 2014) in this case is -8.79 ± 1.1 Tg C yr^{-1}, i.e., an overestimation of 11.0 ± 1.0% (13.8 ± 1.1% on the high-end estimate) by not accounting for the influence of the ITZC in the freshening and fCO_{2sw} dynamics in the Amazon River plume.

3.4. Reevaluating the Sea-Air CO_2 Exchange in the Tropical Atlantic

The mean sea-air CO_2 efflux in the tropical Atlantic (18°S–18°N) is currently estimated to be between 110 Tg C yr^{-1} (reference year 2000 [*Takahashi et al.*, 2009]) and 98 Tg C yr^{-1} (average from 1998 to 2011 [*Landschützer et al.*, 2014]). Both sea-air CO_2 flux climatologies show very similar patterns within the western tropical Atlantic (Figures 3k–3n), with a seasonal role in the area of the North Equatorial Current (from ~12 to ~30°N) and permanent CO_2 efflux near the coast of South America, southeast of the Amazon River mouth (in the area of the oceanic waters transported by the NBC). These CO_2 flux climatologies characterize the area of the Amazon River plume as an almost permanent source of CO_2 to the atmosphere (e.g., Figures 1h, grey dots, and 3k–3n). This contrasts with the results presented here, which are in agreement with early work that recognized the atmospheric C sink associated to the Amazon plume [*Ternon et al.*, 2000; *Körtzinger*, 2003; *Cooley et al.*, 2007]. Furthermore, the climatology of *Landschützer et al.* [2014] is based on the SOCAT database v2, which at the time already included part of the data presented in *Lefèvre et al.* [2010], *Ibánhez et al.* [2015], and this study. The climatology of Takahashi et al. was recently updated for their sea surface pCO_2 values (reference year 2005 [*Takahashi et al.*, 2014]). Although they do not present a climatological atmospheric pCO_2 (and therefore lacks ΔpCO_2 and sea-air CO_2 flux estimations), the updated climatology shows averaged pCO_2 values 6.3 μatm lower than its previous version for the region 2°S–18°N and 60–40°W. Nevertheless, for July, this updated climatology gives pCO_2 values 7.7 μatm higher than the previous version. This is the period of the year when both the area of the Amazon plume and the associated atmospheric CO_2 sink are close to their maximum values (Figures 1g and 1h). Thus, despite previous evidence, these studies have systematically overlooked the impact of the Amazon River plume in the sea-air CO_2 exchange for the region (Figure 3).

To estimate the contribution of the Amazon River plume to the overall sea-air CO_2 exchange in the tropical Atlantic, we used the climatology of *Landschützer et al.* [2014] due to the contemporaneity of their estimations (from 1998 to 2011) with our results and the higher resolution (1°×1°) compared to the climatologies of *Takahashi et al.* [2009, 2014] (4°×5°). Excluding the Caribbean Sea, the climatology of *Landschützer et al.* [2014] gives an estimated net efflux of 90.5 Tg C yr^{-1} for the tropical Atlantic (18°S–18°N). Using the monthly area of the Amazon plume after removing the influence of rainfall, this CO_2 climatology identifies the Amazon River plume as a source of 1.51 ± 0.05 Tg C yr^{-1} (1.42 ± 0.05 Tg C yr^{-1}) to the atmosphere (Figures 1i, grey dots, and 3). This contrasts with the almost permanent CO_2 sink characteristic of the Amazon River plume (Figures 1i, magenta dots, and 3). Based on the calculated annual CO_2 flux within the Amazon plume presented here (from 2011 to 2014) and the CO_2 climatology of *Landschützer et al.* [2014], the CO_2 outgassing in the tropical Atlantic becomes 81.1 ± 1.1 Tg C yr^{-1} (81.5 ± 1.1 Tg C yr^{-1}). According to our results, these estimations of the sea-air CO_2 exchange in the tropical Atlantic would be overestimated by 10.3 ± 1.0% (10.0 ± 1.0%) by overlooking the role of the Amazon River plume.

The sea-air CO_2 flux calculated in this study in the Amazon river plume confirms that this region typically acts as sink for atmospheric CO_2 [*Ternon et al.*, 2000; *Körtzinger*, 2003; *Cooley et al.*, 2007; *Lefèvre et al.*, 2010;

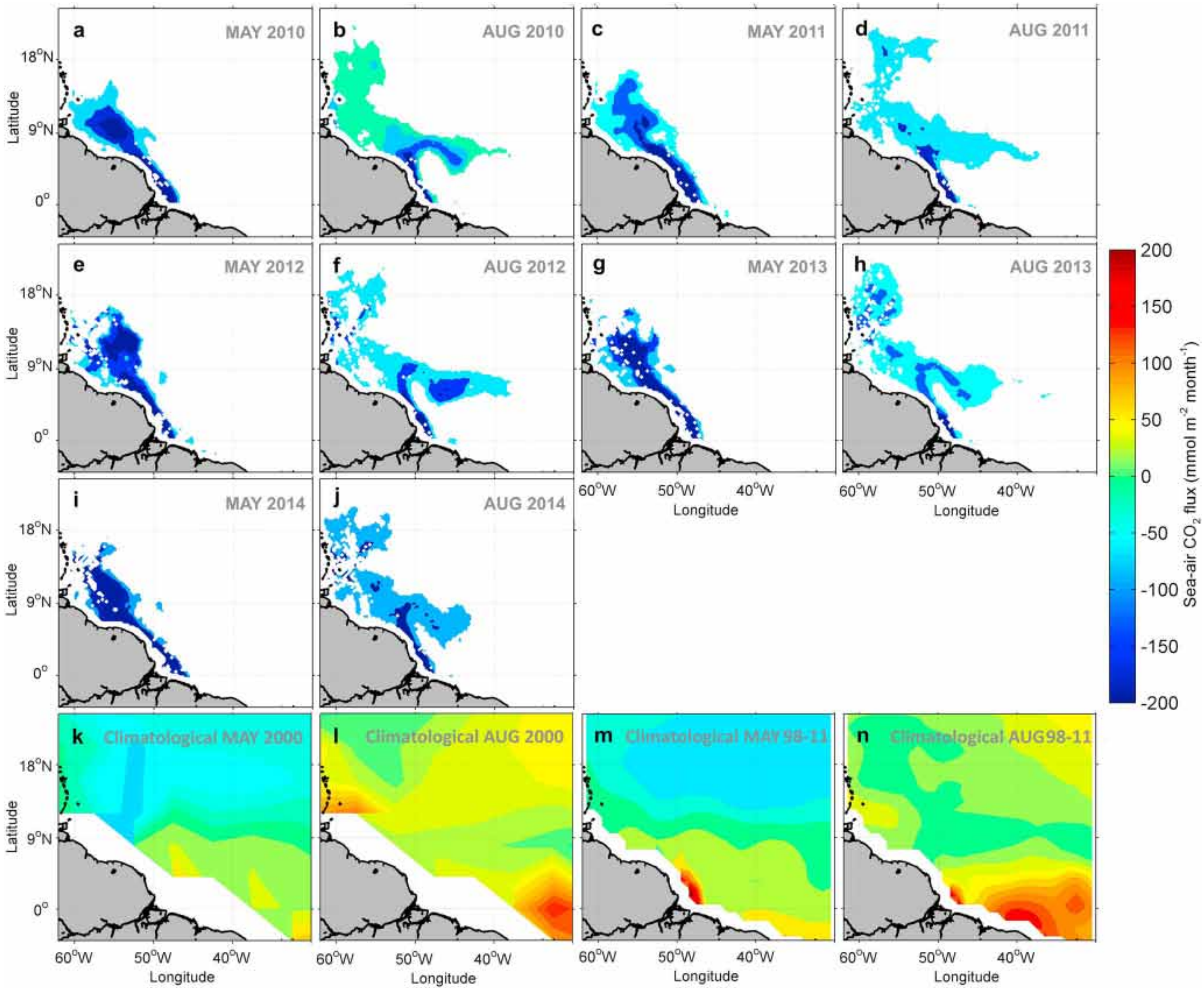

Figure 3. Monthly sea-air CO_2 fluxes in the Amazon River plume area. (a–j) Calculated monthly sea-air CO_2 flux from 2010 to 2014 for May and August within the Amazon plume. The sea-air CO_2 exchange for the western tropical Atlantic as presented in the climatologies of (k and l) *Takahashi et al.* [2009] and (m and n) *Landschützer et al.* [2014] are also presented for May and August for comparison with our results.

Ibánhez et al., 2015] and demonstrates that its CO_2 dynamics can play an important role on the CO_2 balance at regional scale (tropical Atlantic Ocean). Other CO_2 undersaturation zones related to the ITCZ [*Lefèvre et al.*, 2010] or potentially other major rivers discharging into the basin (e.g., Orinoco and Congo) would also have an impact in the net CO_2 flux in the tropical Atlantic. The magnitude of the CO_2 sink associated to these freshwater sources to the basin is expected to be of lower magnitude than that associated to the Amazon River plume due to its disproportionate surface area and the enhanced biological activity associated to it: the area of the Amazon plume is orders of magnitude higher than any other river plume in the world [*Cai et al.*, 2013]. Furthermore, despite the higher extension of the freshening caused by the ITCZ in the tropical Atlantic compared to the Amazon plume, the biological component of its associated sea surface CO_2 undersaturation is minimal [*Lefèvre et al*., 2010]. Yet the CO_2 outgassing in the tropical Atlantic could be lower than currently estimated.

4. Conclusions

Based on empirical relationships between rainfall rate and SSS changes in the tropical Atlantic, we have removed the contribution of the ITCZ to the freshening caused by the Amazon River plume in the western tropical Atlantic. These relationships were also used to calculate the fCO_{2sw} within the Amazon plume without the influence of rainfall over the inorganic C system. These relationships of rainfall versus SSS changes found in this study could also be used in other areas of the tropical Atlantic to remove the freshening caused by the rainfall associated to the ITCZ, such as the Orinoco River plume area.

The influence of the ITCZ on the apparent Amazon plume is revealed to be highly significant, accounting for >16% of the area with bulk SSS <35 in the area. Nevertheless, and after removing also the effect of rainfall over the measured fCO_{2sw} and SSS, this study confirms that the Amazon plume alone is an atmospheric CO_2 sink of global importance (-7.61 ± 1.01 to -7.85 ± 1.02 Tg C yr^{-1}). Based on the results presented here and current sea-air CO_2 climatologies, the sea-air CO_2 exchange for the tropical Atlantic is estimated to be 81.1 ± 1.1 to 81.5 ± 1.1 Tg C yr^{-1}, i.e., about 10% lower than previous estimates by specifically including the Amazon plume in these estimations. Thus, this study emphasizes the need for requantifying the sea-air CO_2 exchange in the tropical Atlantic, by including an explicit representation of river plumes (particularly the Amazon plume due to its disproportionate magnitude), to provide robust quantification of its role at global scale.

Acknowledgments
We acknowledge the Compagnie Maritime Nantaise (MN) for allowing the installation of the CO_2 equipment on board their ship. NCEP Reanalysis-derived data were provided by the NOAA/OAR/ESRL PSD, Boulder, CO, USA (http://www.esrl.noaa.gov/psd/). SSS data derived from thermosalinograph instruments installed onboard voluntary observing ships were collected, validated, archived, and made freely available by the French Sea Surface Salinity Observation Service (http://www.legos.obs-mip.fr/observations/sss/). The LOCEAN_v2013 SSS has been produced by LOCEAN/IPSL that participates in the Ocean Salinity Expertise Center (CECOS) of Centre Aval de Traitement des Données SMOS (CATDS). We thank the support from the European Integrated Projects CARBOOCEAN (contract 511176–2) and CARBOCHANGE (FP7 264879), the Brazilian National Institute of Science and Technology in Tropical Marine Environments, INCT-AmbTropic (CNPq/FAPESB grants 565054/2010-4 and 8936/2011), the BIOAMAZON project, and the Institut de Recherche pour le Developpement (IRD). JSPI was supported by a postdoctoral fellowship from the CARBOCHANGE project. The fCO_2 data presented here are available in the SOCAT v3 database (socat.info). The authors are thankful to S. Pino Groba, Rebecca L. Stirnemann, the editor of GRL, and three anonymous reviewers for their helpful discussions and comments.

References

Abril, G., et al. (2014), Amazon River carbon dioxide outgassing fuelled by wetlands, *Nature*, *505*(7483), 395–398, doi:10.1038/nature12797.
Andrié, C., C. Oudot, C. Genthon, and L. Merlivat (1986), CO_2 fluxes in the tropical Atlantic during FOCAL cruises, *J. Geophys. Res.*, *91*(C10), 11,741–11,755, doi:10.1029/JC091iC10p11741.
Cai, W.-J., C. T. A. Chen, and A. Borges (2013), Carbon dioxide dynamics and fluxes in coastal waters influenced by river plumes, in *Biogeochemical Dynamics at Major River-Coastal Interfaces*, Cambridge Univ. Press, Cambridge, U. K.
Chen, C.-T. A., T.-H. Huang, Y.-H. Fu, Y. Bai, and X. He (2012), Strong sources of CO_2 in upper estuaries become sinks of CO_2 in large river plumes, *Curr. Opin. Environ. Sustain.*, *4*(2), 179–185, doi:10.1016/j.cosust.2012.02.003.
Coles, V. J., M. T. Brooks, J. Hopkins, M. R. Stukel, P. L. Yager, and R. R. Hood (2013), The pathways and properties of the Amazon River plume in the tropical North Atlantic Ocean, *J. Geophys. Res. Oceans*, *118*, 6894–6913, doi:10.1002/2013JC008981.
Cooley, S. R., V. J. Coles, A. Subramaniam, and P. L. Yager (2007), Seasonal variations in the Amazon plume-related atmospheric carbon sink, *Global Biogeochem. Cycles*, *21*, GB3014, doi:10.1029/2006GB002831.
Da-Allada, C. Y., G. Alory, Y. du Penhoat, E. Kestenare, F. Durand, and N. M. Hounkonnou (2013), Seasonal mixed-layer salinity balance in the tropical Atlantic Ocean: Mean state and seasonal cycle, *J. Geophys. Res. Oceans*, *118*, 332–345, doi:10.1029/2012JC008357.
Grodsky, S. A., G. Reverdin, J. A. Carton, and V. J. Coles (2014), Year-to-year salinity changes in the Amazon plume: Contrasting 2011 and 2012 Aquarius/SACD and SMOS satellite data, *Remote Sens. Environ.*, *140*, 14–22, doi:10.1016/j.rse.2013.08.033.
Hernandez, O., J. Boutin, N. Kolodziejczyk, G. Reverdin, N. Martin, F. Gaillard, N. Reul, and J. L. Vergely (2014), SMOS salinity in the subtropical north Atlantic salinity maximum: 1. Comparison with Aquarius and in situ salinity, *J. Geophys. Res. Oceans*, *119*, 8878–8896, doi:10.1002/2013JC009610.
Huffman, G. J., R. F. Adler, D. T. Bolvin, G. Gu, E. J. Nelkin, K. P. Bowman, Y. Hong, E. F. Stocker, and D. B. Wolff (2007), The TRMM Multisatellite Precipitation Analysis (TMPA): Quasi-global, multiyear, combined-sensor precipitation estimates at fine scales, *J. Hydrometeorol.*, *8*, 38, doi:10.1175/JHM560.1.
Ibánhez, J. S. P., D. Diverrès, M. Araujo, and N. Lefèvre (2015), Seasonal and interannual variability of sea-air CO_2 fluxes in the tropical Atlantic affected by the Amazon River plume, *Global Biogeochem. Cycles*, *29*, 1640–1655, doi:10.1002/2015GB005110.
Körtzinger, A. (2003), A significant CO_2 sink in the tropical Atlantic Ocean associated with the Amazon River plume, *Geophys. Res. Lett.*, *30*(24), 2287, doi:10.1029/2003GL018841.
Landschützer, P., N. Gruber, D. C. E. Bakker, and U. Schuster (2014), Recent variability of the global ocean carbon sink, *Global Biogeochem. Cycles*, *28*, 927–949, doi:10.1002/2014GB004853.
Lefèvre, N., G. Moore, J. Aiken, A. Watson, D. Cooper, and R. Ling (1998), Variability of pCO_2 in the tropical Atlantic in 1995, *J. Geophys. Res.*, *103*(C3), 5623–5634, doi:10.1029/97JC02303.
Lefèvre, N., D. Diverrès, and F. Gallois (2010), Origin of CO_2 undersaturation in the western tropical Atlantic, *Tellus B*, *62*(5), 595–607, doi:10.1111/j.1600-0889.2010.00475.x.
Lefèvre, N., G. Caniaux, S. Janicot, and A. K. Gueye (2013), Increased CO_2 outgassing in February-May 2010 in the tropical Atlantic following the 2009 Pacific El Niño, *J. Geophys. Res. Oceans*, *118*, 1645–1657, doi:10.1002/jgrc.20107.
Mignot, J., A. Lazar, and M. Lacarra (2012), On the formation of barrier layers and associated vertical temperature inversions: A focus on the northwestern tropical Atlantic, *J. Geophys. Res.*, *117*, C02010, doi:10.1029/2011JC007435.
Molleri, G. S. F., E. M. L. de M. Novo, and M. Kampel (2010), Space-time variability of the Amazon River plume based on satellite ocean color, *Cont. Shelf Res.*, *30*(3–4), 342–352, doi:10.1016/j.csr.2009.11.015.
Pierrot, D., C. Neill, K. Sullivan, R. Castle, R. Wanninkhof, H. Lüger, T. Johannessen, A. Olsen, R. A. Feely, and C. E. Cosca (2009), Recommendations for autonomous underway pCO_2 measuring systems and data-reduction routines, *Deep Sea Res. Part II Top. Stud. Oceanogr.*, *56*(8–10), 512–522, doi:10.1016/j.dsr2.2008.12.005.
Reynolds, R. W., N. A. Rayner, T. M. Smith, D. C. Stokes, and W. Wang (2002), An improved in situ and satellite SST analysis for climate, *J. Clim.*, *15*, 1609–1625, doi:10.1175/1520-0442(2002)015<1609:AIISAS>2.0.CO;2.
Richey, J. E., J. M. Melack, A. K. Aufdenkampe, V. M. Ballester, and L. L. Hess (2002), Outgassing from Amazonian rivers and wetlands as a large tropical source of atmospheric CO_2, *Nature*, *416*(6881), 617–620, doi:10.1038/416617a.
Richter, I., S. K. Behera, Y. Masumoto, B. Taguchi, H. Sasaki, and T. Yamagata (2013), Multiple causes of interannual sea surface temperature variability in the equatorial Atlantic Ocean, *Nat. Geosci.*, *6*(1), 43–47, doi:10.1038/ngeo1660.
Sarmiento, J. L., and N. Gruber (2006), *Ocean Biogeochemical Dynamics*, Princeton Univ. Press, Princeton, N. J.
Subramaniam, A., et al. (2008), Amazon River enhances diazotrophy and carbon sequestration in the tropical North Atlantic Ocean, *Proc. Natl. Acad. Sci. U.S.A.*, *105*(30), 10,460–10,465, doi:10.1073/pnas.0710279105.
Sweeney, C., E. Gloor, A. R. Jacobson, R. M. Key, G. McKinley, J. L. Sarmiento, and R. Wanninkhof (2007), Constraining global air-sea gas exchange for CO_2 with recent bomb ^{14}C measurements, *Global Biogeochem. Cycles*, *21*, GB2015, doi:10.1029/2006GB002784.
Takahashi, T., et al. (2009), Climatological mean and decadal change in surface ocean pCO_2, and net sea–air CO_2 flux over the global oceans, *Deep Sea Res. Part II Top. Stud. Oceanogr.*, *56*(8–10), 554–577, doi:10.1016/j.dsr2.2008.12.009.

Takahashi, T., S. C. Sutherland, D. W. Chipman, J. G. Goddard, C. Ho, T. Newberger, C. Sweeney, and D. R. Munro (2014), Climatological distributions of pH, pCO_2, total CO_2, alkalinity, and $CaCO_3$ saturation in the global surface ocean, and temporal changes at selected locations, *Mar. Chem.*, *164*, 95–125, doi:10.1016/j.marchem.2014.06.004.

Ternon, J. F., C. Oudot, A. Dessier, and D. Diverres (2000), A seasonal tropical sink for atmospheric CO_2 in the Atlantic Ocean: The role of the Amazon River discharge, *Mar. Chem.*, *68*(3), 183–201, doi:10.1016/S0304-4203(99)00077-8.

Turk, D., C. J. Zappa, C. S. Meinen, J. R. Christian, D. T. Ho, A. G. Dickson, and W. R. McGillis (2010), Rain impacts on CO_2 exchange in the western equatorial Pacific Ocean, *Geophys. Res. Lett.*, *37*, L23610, doi:10.1029/2010GL045520.

Weiss, R. F. (1974), Carbon dioxide in water and seawater: The solubility of a non-ideal gas, *Mar. Chem.*, *2*(3), 203–215, doi:10.1016/0304-4203(74)90015-2.